



ORIGINAL RESEARCH ARTICLE

A pulsed carbon dioxide laser-induced breakdown analysis for chemical profile of tsunami-affected soil

R. Mitaphonna¹, N. Idris^{2,*}, M. Ramli³, N. Ismail², K. Kurihara⁴, K. Lahna²¹ Graduate School of Mathematics and Applied Sciences, Universitas Syiah Kuala, 23111 Banda Aceh, Indonesia² Department of Physics, Faculty of Mathematics and Natural Sciences, Universitas Syiah Kuala, 23111 Banda Aceh, Indonesia³ Department of Chemistry, Faculty of Mathematics and Natural Sciences, Universitas Syiah Kuala, 23111 Banda Aceh, Indonesia⁴ Department of Physics, Faculty of Education, University of Fukui 3-9-1, Bunkyo, Fukui 910-8507, Japan

ARTICLE INFO

Article History:

Received 27 December 2023

Revised 02 March 2024

Accepted 10 April 2024

Keywords:

Calibration-free laser-induced
breakdown spectroscopy (CF-
LIBS)

Chemical Profile

Pulsed carbon dioxide (CO₂) laser

2004 Indian Ocean tsunami

Aceh Province

ABSTRACT

BACKGROUND AND OBJECTIVES: The catastrophic 2004 Indian Ocean tsunami left a profound mark, triggering significant contamination of organic and inorganic chemical components in the water and soil of affected regions. The effects of the tragedy, which occurred almost twenty years ago, are still evident in the soil as salt and metal pollutants continue to linger. It is crucial to conduct a chemical analysis of the soil samples obtained from the regions affected by the Indian Ocean tsunami in 2004. This not only aids in identifying areas hit by the catastrophe but also facilitates periodic monitoring of chemical contamination levels. This study aims to promptly detect and measure chemical indicators in soil samples collected from areas in Aceh Province that were impacted by the 2004 Indian Ocean tsunami.**METHODS:** Three regions in Aceh Province, specifically Banda Aceh, Aceh Besar, and Aceh Barat, were selected for the collection of soil samples following severe impact from a tsunami. Soil samples were obtained from regions unaffected by the tsunami, including Tungkob, Blang Bintang, and Pango Deah. Plasma was produced by concentrating a pulsed carbon dioxide laser beam on the surface samples. An optical multichannel analyzer captures plasma emissions with a spectrograph and photodiode array. Data is stored for processing with SpectraView software and compared with the National Institute of Standards and Technology database for identification.**FINDINGS:** The utilization of a pulsed carbon dioxide laser for analysis revealed its superior ability to identify a wider array of elements with high intensity-to-background ratios, particularly excelling in the detection of zinc, chromium, copper, cobalt, and nickel compared to the neodymium-doped yttrium aluminum garnet laser. Chemical quantification through calibration-free laser-induced breakdown spectroscopy closely correlated with x-ray fluorescence but surpassed x-ray fluorescence in rapid detection and identification of lighter elements. The concentrations of salt components and particular heavy metals in soil that was impacted by a tsunami exhibited a more than tenfold increase in comparison to soil that was not affected and was collected in 2006. Sodium surged from 0.02 percent to 4.18- 4.95 percent, while calcium increased from 0.46 percent to 11.26 - 13.53 percent. Potassium concentration rose from 0.11 percent to 5.50- 6.96 percent, alongside magnesium, which increased from 0.36 percent to 7.62- 8.67 percent.**CONCLUSION:** The utilization of a pulsed carbon dioxide laser-induced breakdown spectroscopy has demonstrated remarkable proficiency in the identification of a diverse range of elements. This technique has surpassed conventional methods like neodymium-doped yttrium aluminum garnet laser-induced breakdown spectroscopy, energy dispersive spectroscopy, and x-ray fluorescence in terms of its detection capabilities. This study underscores the potential of a pulsed carbon dioxide laser as a versatile and reliable method for qualitative and quantitative analysis of soils from 2004 Indian Ocean tsunami-affected regions in Aceh Province, emphasizing its significance for environmental monitoring in disaster-affected areas.DOI: [10.22034/gjesm.2024.03.17](https://doi.org/10.22034/gjesm.2024.03.17)This is an open access article under the CC BY license (<http://creativecommons.org/licenses/by/4.0/>).

NUMBER OF REFERENCES

38



NUMBER OF FIGURES

8



NUMBER OF TABLES

3

*Corresponding Author:

Email: nasrullah.idris@usk.ac.id

Phone: +6281 26945 7430

ORCID: [0000-0002-1650-8365](https://orcid.org/0000-0002-1650-8365)

Note: Discussion period for this manuscript open until October 1, 2024 on GJESM website at the "Show Article".

INTRODUCTION

The destructive tsunami in 2004, which was initiated by a potent underwater earthquake, caused extensive devastation and casualties in 14 countries along the Indian Ocean coastline. Aceh Province, situated on the western coast of Indonesia, stands out as one of the hardest-hit regions by tsunami disaster, leaving countless buildings and infrastructure reduced to rubble and claiming the lives of hundreds of thousands. The tsunami led to the pollution of different chemical substances, specifically dangerous heavy metals and organic compounds in regions affected by the tsunami (Chagué-goff *et al.*, 2017; Daly *et al.*, 2017; Shinozaki, 2021; Shinozaki *et al.*, 2022). The presence of these chemicals presents a notable threat to both the ecosystem and public well-being, exacerbated by the possibility of polluting water sources, seafood, or encountering harmful agents directly (Zakaly *et al.*, 2021; Sulistyowati *et al.*, 2023). Consequently, in order to combat chemical contamination in regions impacted by the tsunami, it is essential to systematically detect and analyze the chemical elements found in the soil affected by the 2004 Indian Ocean tsunami. Such analysis plays a critical role in bolstering ecosystem restoration and recovery endeavors, deepening geological insights and records, and furnishing indispensable data for crafting effective preventive strategies against potential future chemical contamination (Ishizawa *et al.*, 2019; Watanabe *et al.*, 2022). Various analytical methods have been utilized to identify and measure the chemical makeup of samples. These techniques encompass ion chromatography (IC), flame atomic absorption spectrometry (FAAS), inductively coupled plasma (ICP), instrumental neutron activation analysis (INAA), x-ray fluorescence (XRF), and energy dispersive x-ray spectroscopy (EDS) (Messenger *et al.*, 2021; Philip and Singh, 2020; Ravansari *et al.*, 2020). Despite their versatility, these methodologies often involve intricate sample preparation procedures, extensive time and energy consumption, and the use of hazardous solvents (Liu *et al.*, 2015; Tripathi *et al.*, 2015). Prior studies have identified constraints in the effectiveness of EDS and XRF techniques when examining the chemical makeup of soil affected by tsunamis. Specifically, these methods have proven to be inadequate in detecting low molecular weight elements, which are essential for analyzing intricate soil samples (Idris *et al.*, 2022; Mitaphonna *et al.*, 2023). Consequently,

there arises a critical need for rapid and efficient tools to comprehensively analyze the chemical composition of soil affected by tsunamis. Laser-induced breakdown spectroscopy (LIBS) is an innovative analytical technique that utilizes pulsed lasers to atomize substances and generate characteristic spectral lines of elements for rapid qualitative and quantitative analysis (Brunnbauer *et al.*, 2023; Legnaioli *et al.*, 2020; Yu *et al.*, 2020). LIBS is distinguished from other elemental analysis methods by its unique ability to access almost the entire periodic table of elements. This exceptional feature allows for accurate measurement of low-molecular-weight elements that are difficult to detect using alternative analytical techniques (Zivkovic *et al.*, 2018; Villas-Boas *et al.*, 2020). Extensive study has been conducted on soil analysis utilizing LIBS in agriculture and geographical distribution. However, the unique aspect of this study is the utilization of a pulsed carbon dioxide (CO₂) LIBS technique to analyze the chemical compositions of soil collected from tsunami-affected areas in Aceh Province. The pulsed CO₂ laser can generate a larger plasma volume due to its longer wavelength, making it easier to detect elements and compounds across a broader spectral range, particularly trace elements (Khumaeni *et al.*, 2022). In contrast to the neodymium-doped yttrium aluminum garnet (Nd-YAG) laser, unlike its counterpart, presents difficulties in analyzing heavy metal traces due to its high photon energy, resulting in less effective atomization of these elements. The utilization of pulsed CO₂ lasers can enhance the protective plasma effect, resulting in a more stable and intense plasma formation, thereby improving the quality of the spectroscopic analysis obtained (Khumaeni *et al.*, 2018, 2020). Furthermore, this research employs the calibration-free laser-induced breakdown spectroscopy (CF-LIBS) method to quantify the chemical constituents in tsunami-impacted soil. CF-LIBS offers a variety of benefits, such as non-destructive analysis, rapid results, simplified sample preparation, and the ability to analyze multiple elements concurrently (Fayyaz *et al.*, 2023). This study signifies a preliminary stage in the implementation of the CF-LIBS technique for evaluating the chemical makeup of soil collected from regions impacted by the 2004 Indian Ocean tsunami. The aims of this study are two-fold: firstly, to enhance and refine the pulsed CO₂ LIBS technique for comprehensive analysis of chemical constituents, encompassing salt elements, metals and heavy metals, trace elements, and organic compounds

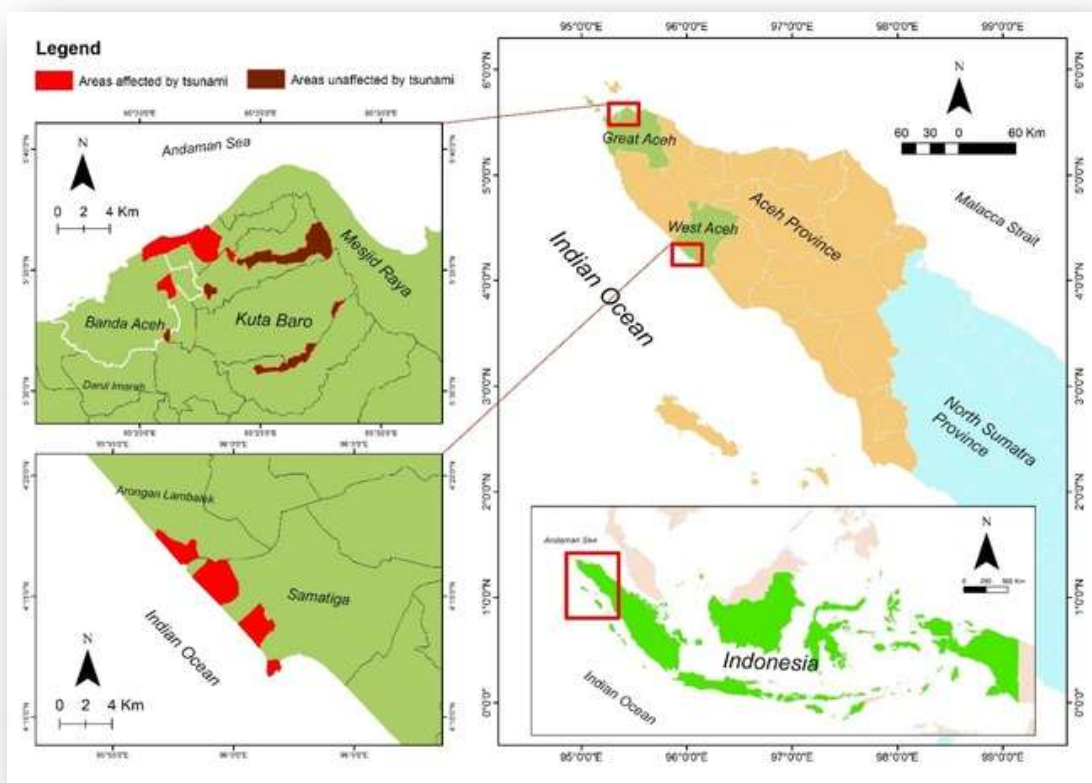


Fig. 1: Geographic location of the study area in Indian Ocean tsunami in Aceh Province, Indonesia along with the sampling locations of the impacted and unimpacted soil by 2004

in soil samples from tsunami-affected regions in Aceh Province, Indonesia. Secondly, to quantify the chemical composition of soil sampled from tsunami-affected regions, utilizing the CF-LIBS method. This study was carried out in Aceh Province, Indonesia, in 2022.

MATERIALS AND METHODS

Sample collection

Soil samples were collected from three heavily affected areas in Aceh Province post-tsunami: Banda Aceh City, Aceh Besar, and Aceh Barat Regencies (Fig. 1). In Banda Aceh City, samples were taken from three locations (Banda Aceh 4, 5, and 8), labeled A, B, and C, respectively. In Aceh Besar Regency, samples were obtained from four sites (Aceh Besar 1, 2, 3, and 9), labeled D, E, F, and G. Aceh Barat Regency sampling comprised four points (Kampung Cot 4, 5, 6, and 7), labeled H, I, J, and K. Soil samples unaffected by the tsunami were collected from

Tungkob, Pango Deah, and Blang Bintang, marked as L, M, and N, respectively. The samples were gathered from marshes or neglected agricultural areas to retain traces of tsunami sediment. The depth at which soil was collected to address post-tsunami contamination was 10 centimeters (cm), employing a vertical insertion method with a hand auger. The identification of tsunami sediment was accomplished through the Troels-Smith classification. Sample preparation involved removing organic materials, drying them at 105 degrees Celsius (°C) for 1 hour (h), and compressing them into pellets using a hydraulic press (5 tons pressure) resulting in pellets 0.7 cm wide and 0.6 cm thick.

A pulsed CO₂ LIBS experimental setup

The illustration of the LIBS setup is presented in Fig. 2, which includes a pulsed CO₂ laser with specifications: 10.6 micrometers (μm) wavelength,

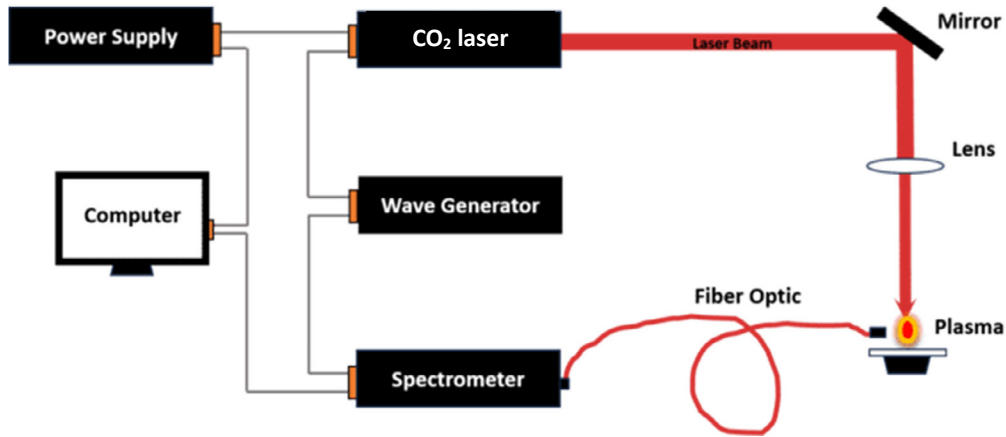


Fig. 2: Schematic of a pulsed CO₂ laser setup employed for the analysis of soil samples

200 nanoseconds (ns) pulse duration, and 10 Hertz (Hz) frequency. An Optical Multichannel Analyzer (OMA) utilized an optical detector consisting of a spectrograph with a focal length of 0.32 m, a grating with 1200 grooves/mm, and a photodiode detector array with 1024 channels, along with a microchannel plate amplifier. Plasma induction was achieved by precisely directing a pulsed CO₂ laser beam onto the surface of a pellet housed within a coiled metal chamber, employing a zinc selenide (ZnSe) lens. The plasma emissions were captured by the OMA system, following which the emitted light was directed into the spectrometer input via an optical fiber. The photodiode array successfully captured the optical signal, while the OMA system, coupled with a computer running SpectraView software, stored the collected data for future analysis. The resultant was subjected to a thorough comparison with the database of the National Institute of Standards and Technology (NIST) in order to facilitate identification.

CF-LIBS analysis

Elemental content analysis utilized CF-LIBS with a single calibration method (Ciucci *et al.*, 1999). The total intensity of detected element emission lines was determined using Eq. 1 (Aldakheel *et al.*, 2021).

$$I = FC_s A_{ki} \frac{g_k}{U(T)} \exp\left(\frac{-E_k}{kT}\right) \quad (1)$$

The next step involves deriving the F parameter by standardizing the concentrations of all constituent species, using Eqs. 2 and 3 (Aldakheel *et al.*, 2021):

$$\sum_s \bar{C}_s = \frac{1}{F} U_s(T) \exp(q_s) = 1 \quad (2)$$

$$q_s = \ln\left(\frac{C_s(F)}{U(T)}\right) \quad (3)$$

Species concentration in soil samples can be acquired using Eq. 4 (Aldakheel *et al.*, 2021):

$$C_s = \frac{1}{F} U_s(T) \exp(q_s) \quad (4)$$

The abundance of neutral, singly-ionized, and doubly-ionized species, governed by Equation (5), relies on the sample's elemental concentration (Aldakheel *et al.*, 2021):

$$C_{i(\text{tot})} = C_s(\text{I}) + C_s(\text{II}) \quad (5)$$

RESULTS AND DISCUSSION

Optimization of laser parameters and verifying the local thermodynamic equilibrium of plasma

Accurate adjustment of laser pulse energy is essential in this study to prevent impeding ablation rates and plasma density, consequently impacting local thermodynamic equilibrium (LTE). Optimal pulse energy ensures the establishment of LTE without generating excessively intense plasma, which could reabsorb emitted atomic radiation and diminish LIBS signal intensity. It is crucial to modify the delay time in order to improve the sharpness of emission lines. According to the study results, a delay time of 2 microseconds (μs) is considered ideal for the majority

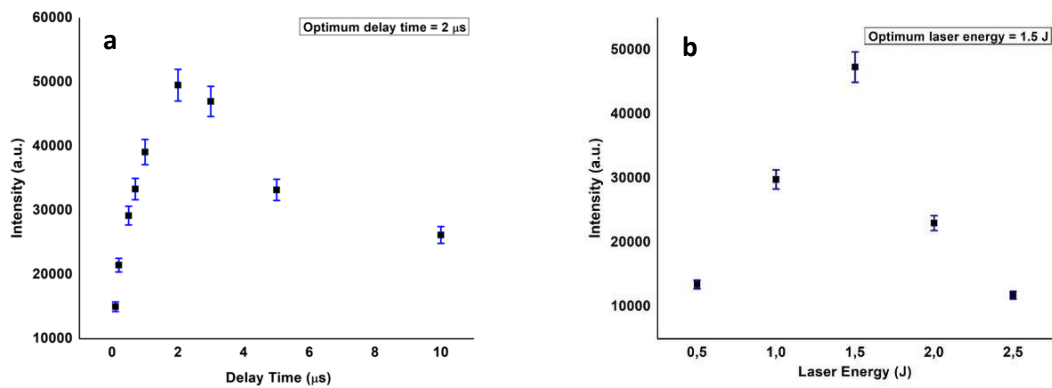


Fig. 3: The impact of (a) delay time and (b) laser energy variation on LIBS signal intensity utilizing the neutral calcium atom line at a wavelength of 422.6 nm

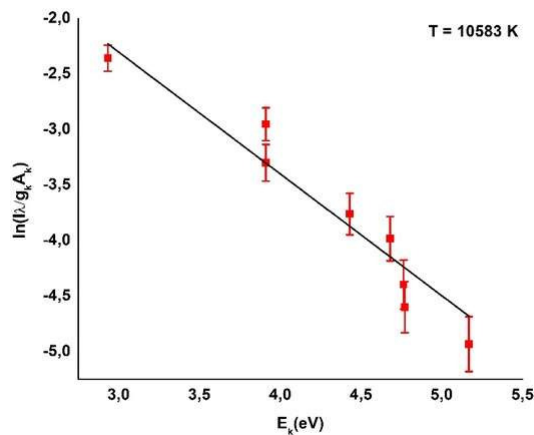


Fig. 4: A linear Boltzmann plot of calcium ion (Ca II) emission lines for estimating the plasma

of identified elements, particularly calcium (Ca) at 422.6 nanometers (nm) (Fig. 3a). Experimental trials show a direct correlation between increasing pulse energy and Ca I emission line intensity, reaching an optimal intensity of around 1.5 Joules (J) per pulse (Fig. 3b).

Studying plasma properties like electron temperature (T_e) and electron density (N_e) is crucial for understanding plasma dynamics in tsunami-affected soil samples (Rehan *et al.*, 2021). Laser-induced plasma (LIP) collisions facilitate the equilibrium of energy dissipation, enabling a comprehensive examination of plasma properties. LIP is found to be in a state of LTE, indicating minimal plasma thickness and negligible self-absorption effects. The minimum threshold for electron density in soil samples affected by tsunamis is established based on McWhirter's

criteria. Meanwhile, the electron temperature is typically calculated through the Boltzmann plot method, which involves identifying suitable spectral transitions related to the element under investigation. A linear Boltzmann plot using Ca transition lines yields an electron temperature of 10.583 Kelvin (K). The robust coefficient of determination ($R = 0.89$) signifies a remarkable concordance with spectroscopic information, affirming strict adherence to LTE conditions (Fig. 4).

The temperature of tsunami-affected soil The determination of plasma electron density is accomplished through the analysis of the Full Width at Half Maximum (FWHM) of isolated, ionized single transitions, employing the Stark broadening technique. Electron density is estimated by observing the Ca I line at 422.5 nm, which displays a distinct Lorentzian

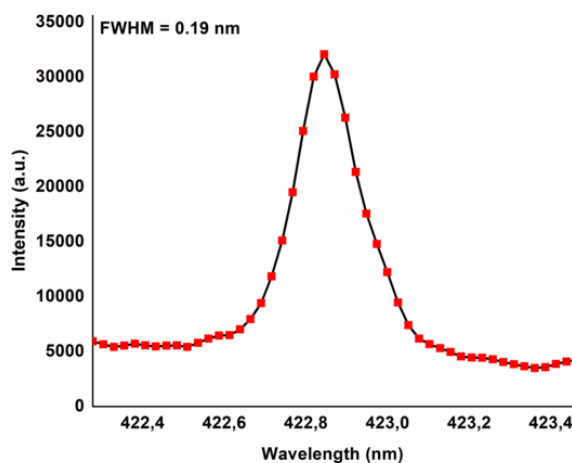


Fig. 5: Stark broadening profile of Ca I 422.5 nm for estimating electron density

profile (Fig. 5). The absence of self-absorption effects is confirmed by the precise conformity of the Ca I line at 422.5 nm with the Lorentzian pattern. With a calculated electron density of $3.97 \times 10^{18} \text{ cm}^{-3}$ based on the FWHM value and Stark broadening parameter estimate, it is notably below the previously estimated lower limit of $4.20 \times 10^{15} \text{ cm}^{-3}$. This underscores the scarcity of observed plasma and its adherence to LTE conditions, minimizing spectral line distortion due to self-absorption effects.

Qualitative and quantitative analysis of soil sampled from tsunami impacted regions

The areas affected by the tsunami are divided into three categories based on the severity of impact: severe, moderate, and minor, which are determined by the extent of damage and casualties. This classification is derived from an assessment of geographical features, infrastructure, and casualty figures in each affected area. Aceh Province is distinguished as one of the regions that has been greatly affected, experiencing substantial destruction and a significant number of casualties (Wisner et al., 2004). A macroscopic analysis by Troels-Smith was carried out prior to conducting LIBS analysis on soil in areas affected by a tsunami. The soil in these areas displayed a distinct bright grey coloration and showed gradual transitions in grain size. Additionally, the presence of wood chips, roots, and rocks was observed in the soil. The delineation between this soil and the adjacent layers was distinct, confirming the influence of the tsunami. Unaltered soil in different regions

exhibited a deep brown hue, consistent grain size, and a lack of organic material. The CO_2 LIBS analysis indicates that numerous chemical elements were detectable in both tsunami-affected and unaffected soil samples (Fig. 6), including salt elements such as Ca, aluminum (Al), magnesium (Mg), sodium (Na), and potassium (K), metals and heavy metals such as titanium (Ti), iron (Fe), silicon (Si), barium (Ba), strontium (Sr), manganese (Mn), chromium (Cr), zinc (Zn), lead (Pb), copper (Cu), cobalt (Co), and nickel (Ni), as well as organic elements, carbon (C), hydrogen (H), oxygen (O), and nitrogen (N). The soil samples collected from regions affected by tsunamis exhibited higher emission intensities for all observed elements, suggesting elevated concentrations in those samples. This observation aligns with previous research, which has consistently demonstrated that tsunamis can induce substantial alterations in the chemical makeup of soil. The application of EDS and XRF revealed the presence of higher levels of seawater elements (Na, Ca, Mg, K, Al, and Si), terrestrial components (Ti and Fe), and organic compounds (C and O) in tsunami-affected soil samples (Mitaphonna et al., 2023). A previous investigations into tsunami-affected soil in Aceh Province using Nd-YAG LIBS only focused on three elements, namely Fe, Ti, and Mg (Idris et al., 2022). The investigations conducted thus far have failed to provide a thorough analysis of every component present in soil samples taken from regions impacted by tsunamis, despite the presence of a wide range of substances, such as dangerous heavy metals. In this research, a pulsed CO_2 LIBS demonstrated

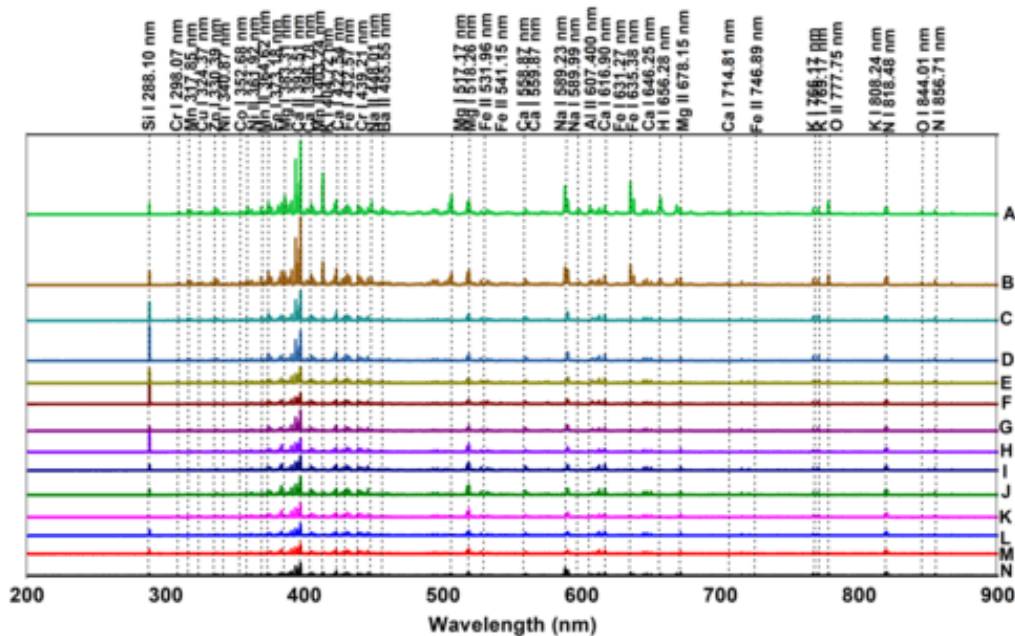


Fig. 6: The emission spectrum lines of affected and unaffected soil samples collected from various areas in Aceh Province were analyzed within the wavelength range of 200-900 nm

its capability to identify a broader spectrum of chemical elements, including organic elements and various heavy metals, previously inaccessible by EDS and XRF. A pulsed CO₂ LIBS also can detect a wider range of emission lines from both neutral and ionic atoms, particularly heavy metals (Zn, Cr, Cu, Co, dan Ni), which are beyond the reach of Nd-YAG LIBS. The pulsed CO₂ LIBS exhibits higher emission intensity and lower background noise levels in its analytical spectrum when compared to Nd-YAG LIBS. A pulsed CO₂ LIBS outperforms several conventional techniques mentioned previously. Pulsed CO₂ LIBS provides improved spectral resolution, enabling precise identification of emission lines from a variety of elements. It boasts exceptional sensitivity, capable of detecting element concentrations at levels as low as parts per million (ppm) or even lower, outperforming conventional chemical techniques that require intricate sample preparation procedures (Khan *et al.*, 2022). Pulsed CO₂ LIBS provides improved spectral resolution, enabling precise identification of emission lines from a variety of elements. It boasts exceptional sensitivity, capable of detecting element concentrations at levels as low as parts per million (ppm) or even lower, outperforming conventional

chemical techniques that require intricate sample preparation procedures. CO₂ LIBS emerges as a superior technique in chemical composition analysis due to its numerous advantages. It excels in the detection of low molecular weight elements and specific metals, making it highly effective in this regard. To ensure accurate observation, the wavelength range was systematically narrowed down by 10 nm increments. Salt elements such as Ca and Al were detected at wavelengths, Ca II 393.36 nm, Al I 394.40 nm, Al I 396.15 nm, and Ca II 396.84 nm (Fig. 7a). Mg emission lines (Mg I 516.94 nm, Mg I 517.44 nm, Mg I 518.68 nm) are visible in the 510 - 520 nm spectrum (Fig. 7b). Na exhibits two emission lines at 588.99 nm and 589.59 nm (Fig. 7c), while K emission lines are sobserved at 404.72 nm and 766.10 nm (Fig. 7d). These spectra exhibit greater intensity and reduced levels of background noise compared to earlier studies on Nd-YAG laser. In the 330 nm to 340 nm range, Zn emission lines at 330.39 nm and 333.34 nm, along with Cr II at 332.42 nm and 334.32 nm, were detected. Ti exhibited four emission lines at 335.05 nm, 336.23 nm, 337.40 nm, and 338.48 nm (Fig. 8a). Fe emission lines were detected in the wavelength range of 370 nm to 380 nm (Fig. 8b). Mn

Soil sampled from tsunami-impacted regions

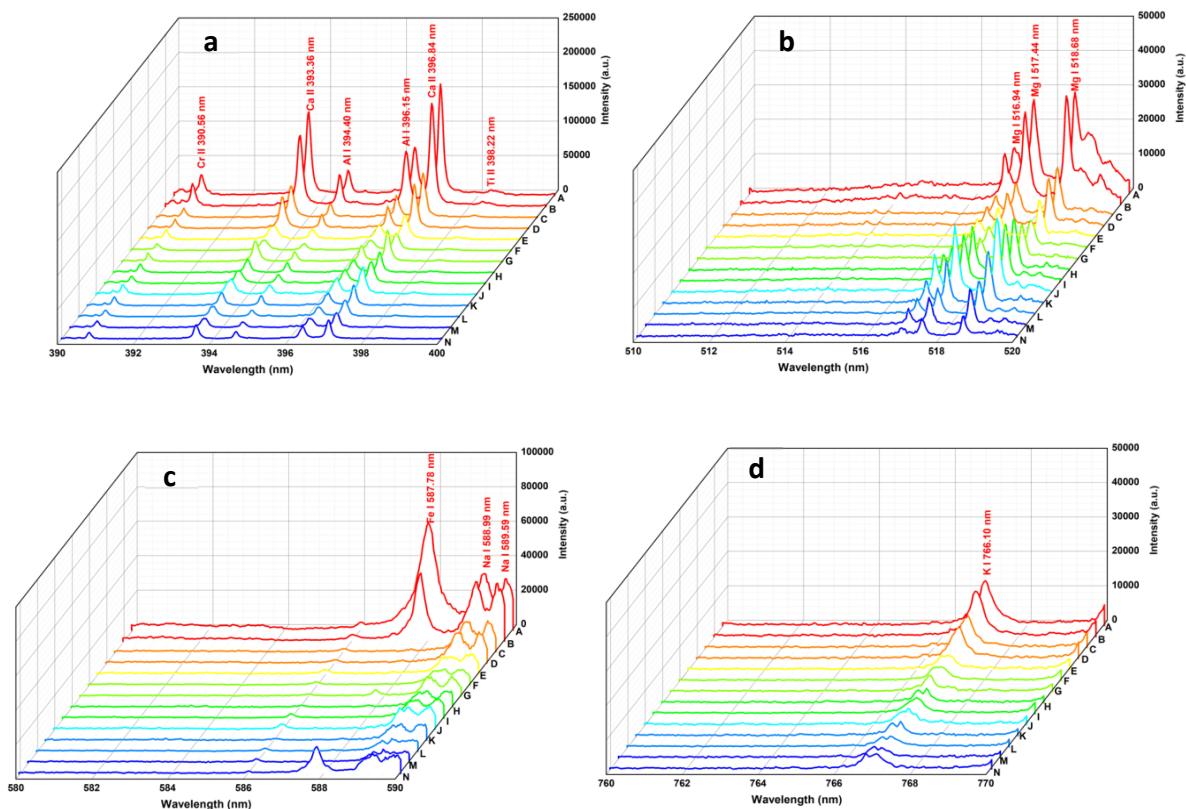


Fig 7. The emission spectrum lines of soil samples affected and unaffected by the 2004 Indian Ocean tsunami in several regions of Aceh Province across the wavelength ranges (a) 390-400 nm, (b) 510-520 nm, (c) 580-590 nm, and (d) 760-770 nm

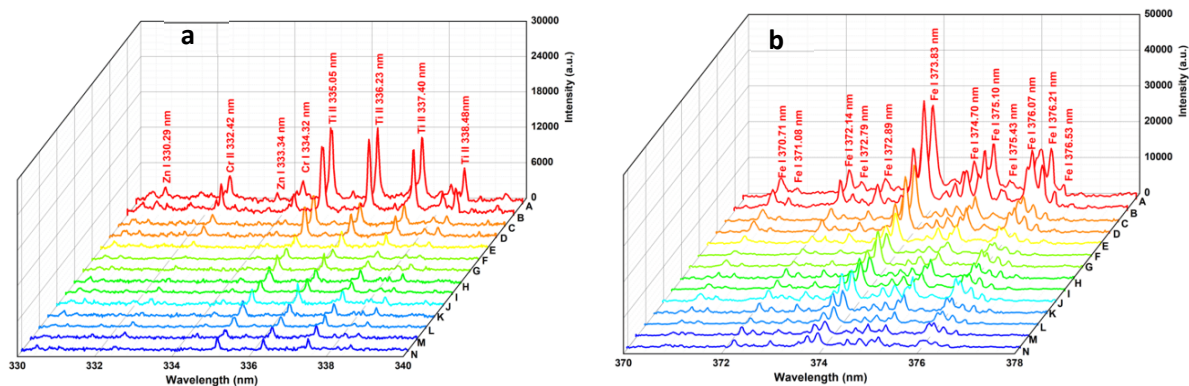


Fig. 8: The emission spectrum lines of soil samples affected and unaffected by the 2004 Indian Ocean tsunami in several regions of Aceh Province across the wavelength ranges (a) 330-340 nm, and (b) 370-378 nm

emission lines appeared at 425.60 nm, 427.35 nm, and 428.45 nm, while Ba and Sr were detected at 455.55 nm and 460.88 nm, respectively. Cu, Ni, and Co were also identified using pulsed CO₂ LIBS, with Cu I lines observed at 324.37 nm, 324.97 nm, and 326.27 nm,

Ni I lines at 340.87 nm and 344.21 nm, and Co lines at 352.68 nm and 356.97 nm. Organic elements including C, H, O, and N were detected across all samples, with C observed at 247.7 nm, H at 656.21 nm, two N lines at 818.88 nm and 821.63 nm, and O at 777.19 nm.

Table 1: The comparative results of chemical element concentrations in both soils sampled from tsunami-affected and unaffected areas were obtained through CF-LIBS and XRF analysis

Elements	Concentration (%)									Unaffected soil ¹
	Banda Aceh 4 (A)			Aceh Besar 2 (E)			Kampong Cot 6 (J)			
	CF-LIBS	XRF	Missmatch (%)	CF-LIBS	XRF	Missmatc h (%)	CF-LIBS	XRF	Missmatc h (%)	
Ca	13.53	-	-	13.17	-	-	11.26	-	-	0.46
K	6.96	-	-	7.98	-	-	5.60	-	-	0.11
Mg	8.67	-	-	7.59	8.85	-	7.62	6.00	0.27	0.36
Na	4.95	-	-	4.40	-	-	4.18	-	-	0.02
Al	7.97	-	-	7.55	8.55	0.14	7.93	8.63	0.08	5.08
Si	16.57	18.2	-	15.58	17.46	-	14.49	16.02	0.10	0.25
Fe	7.34	-	-	5.62	6.6	0.12	7.67	8.69	0.12	3.25
Ti	2.98	3.44	-	2.50	2.89	0.11	2.36	2.45	0.04	-
Ba	1.71	-	-	1.94	-	0.15	1.82	-	-	-
Sr	1.99	-	-	2.02	-	0.13	1.59	-	-	0.02
Co	0.77	1.37	0.44	0.66	-	-	0.40	-	-	0.002
Cu	0.83	1.51	0.45	0.79	1.66	-	0.41	-	-	0.003
Cr	0.97	1.56	0.38	1.09	1.75	-	1.15	1.92	0.40	0.01
Pb	1.86	2.53	0.26	1.77	-	0.52	1.74	2.02	0.14	0.001
Mn	2.71	2.46	0.10	1.90	2.29	0.38	1.18	1.42	0.17	0.04
Ni	0.86	1.48	0.42	0.92	1.77	-	1.09	1.75	0.38	0.005
Zn	0.76	1.38	0.45	0.69	-	-	0.78	1.53	0.49	0.01
C	4.21	-	-	6.90	-	-	5.84	-	0.27	1.2
H	2.26	-	-	3.27	-	-	2.30	-	-	0.1
O	8.67	-	-	9.01	-	-	11.03	-	0.08	-
N	5.41	-	-	5.00	-	-	4.13	-	0.10	-

Data not shown in this manuscript. The utilization of pulsed CO₂ LIBS technology carries significant implications for understanding the chemical changes and consequences caused by tsunamis, specifically in relation to soil composition. CO₂ LIBS facilitates in-depth examinations, allowing for a comprehensive investigation of the relative concentrations of elements and their spatial distributions in samples. This analytical technique offers valuable insights into the influence of natural disasters on soil chemistry and reveals potential patterns underlying these impacts. The improved comprehension of changes in soil components following a tsunami provides a strong basis for developing better mitigation plans, directing specific actions to recover environmental health, and supporting ecosystem rehabilitation following calamities. A pulsed CO₂ LIBS provides extensive information regarding the environmental consequences of tsunamis, while also facilitating the implementation of proactive and effective strategies to ensure environmental sustainability in the future.

Quantitative analysis of chemical elements in soil sampled from tsunami affected regions (Banda Aceh

4, Aceh Besar 2, and Aceh Barat 6) was conducted using CF-LIBS and XRF (Table 1). CF-LIBS stands out for its numerous advantages over traditional calibration curve methods in chemical analysis. An important benefit is its ability to produce immediate quantitative analysis outcomes without requiring the creation of a detailed calibration curve, thus conserving precious time and resources during sample testing (Hu *et al.*, 2022). CF-LIBS takes advantage of a broader spectrum of data obtained from the plasma emission of the sample, enabling the identification of elements that may go unnoticed in traditional calibration curves (Martínez-Mincheró *et al.*, 2022; Quackatz *et al.*, 2024). XRF was incorporated to cross-validate and ensure consistency with the results obtained from CF-LIBS analysis, given its established reputation in elemental composition analysis. Although there are slight differences in concentration between CF-LIBS and XRF, usually ranging from 0.4% to 0.6%, the results obtained from CF-LIBS closely resembled those obtained from traditional XRF calculations. CF-LIBS revealed a significant prevalence of Si, ranging from 14.49 to 16.57% in tsunami-affected

soil, followed by salt elements (Ca, Mg, Al, K, and Na). The concentrations of metals and heavy metal elements remained below 3%. A pulsed CO₂ LIBS excels in detecting a wide array of elements, including salt constituents, various metals, heavy metals, and organic components, surpassing the limited capability of XRF, which struggles with low-molecular-weight organic elements due to technical constraints. A comparative analysis was carried out to evaluate the soil conditions before and after the tsunami by utilizing soil samples collected in 2006 from regions that were not impacted by the tsunami in a prior study (Chaerun et al., 2009). The soil samples were collected from a significant distance away from the coastline, specifically around 13.6 kilometers, thus making them suitable representatives of the soil conditions prior to the occurrence of the tsunami. One of the significant changes observed in the soil affected by the tsunami is the notable rise in the levels of salt elements, including Na, Ca, K, and Mg. The concentration of Na in unaffected soil surged from 0.02% to 4.18 - 4.95% in affected soil. Ca concentration witnessed a substantial rise from 0.46% to 11.26 - 13.53%. There was a significant elevation in K concentration from 0.11% to 5.50 - 6.96%, alongside Mg concentration climbing from 0.36% to 7.62 - 8.67%. The modifications indicate the intrusion of ocean water onto the terrestrial surface as a result of the tsunami, carrying a substantial amount of salts and minerals. Na, a predominant component of seawater, demonstrates a notable surge in its concentration in the tsunami-affected soil. A tsunami not only brings an intrusion of seawater rich in salt and minerals onto the land but also induces coastal erosion, transporting marine sediment material to the affected areas. This process enhances the content of salt and minerals in the soil through sediment deposition (Shinozaki et al., 2021). The tsunami also plays a role in the rise of these elements' concentration by causing damage to vegetation, which in turn leads to the decomposition of organic matter. This process ultimately strengthens the soil's ability to retain salt and minerals. The concentration of Al showed an increase from 5.08% to 7.55-7.97%. The rise in Al concentration could be attributed to significant soil erosion as a result of the tsunami impact. In unaffected soil sampled in 2006, the concentrations were 3.25% for Fe, 0.04% for Mn, and 0.01% for Zn. However, in soil sampled

in tsunami-impacted regions, the concentrations spiked to 7.34% for Fe, 2.71% for Mn, and 0.86% for Zn. The abrupt surge in quantities may point to the presence of heavy metals deposited by the tsunami-affected seawater, causing a shift in the elemental structure of the soil. The concentration of organic C increased notably from 1.2% to 8.67%, with a rise in H concentration from 0.1% to 5.41%. This significant surge is attributed to the influx of organic materials from external sources, such as plants or other organic matter transported by the tsunami. The inputs play a crucial role in shaping alterations in soil composition and chemistry. Consequently, it can be deduced that despite the passage of nearly two decades since the tsunami, the levels of salt, heavy metals, and organic components in the soil affected by the tsunami persistently remain elevated. The tsunami event not only caused detrimental effects on the flooded areas, such as elevated levels of salt and heavy metals, but also resulted in some positive impacts. The increased presence of micronutrients and macronutrients within organic carbon contributes to mitigating salt and heavy metal pollution in the soil. This study aligns with prior research, following the tsunami, the concentrations of salts and metals in agricultural land in Banda Aceh City experienced a significant increase. The tsunami-affected soil was contaminated by heavy metals (Cr, Fe, Co, Ni, Cu, Zn, Mn, cadmium (Cd), Pb) and salts (K, Ca, Mg, Na). Even after 3.5 years of bioremediation efforts, the concentrations of heavy metals in the tsunami-affected soil remained higher (Chaerun et al., 2009). Another study, reported by Szczucinski et al., (2007), further highlights that soil in Thailand post-tsunami exhibits remarkably high concentrations of salts (Na, K, Ca, Mg) and heavy metals (Cd, Cr, Ni, Cu, Zn, and Pb). Following the occurrence of tsunami waves, there was a marked elevation in the levels of certain elements such as Ca, Fe, Sr, S, Ti, and Zr in the chemical composition of sediment found in the Miyazaki Lowlands, Japan. (Watanabe et al., 2022).

Comparison of LIBS signal emission intensity with chemical indicators

An assessment was also carried out on the ratios of emission line intensity for different elements present in the soil samples, owing to the significant correlation between spectral emission line intensity and the concentration of analytes in the sample

(Tables 2 and 3). A range of intensity ratios, including Na/Ti, Ca/Ti, magnesium over titanium (Mg/Ti), aluminum over titanium (Al/Ti), Si/Ti, calcium over iron (Ca/Fe), calcium over magnesium (Ca/Mg), calcium over kalium (Ca/K), barium over strontium (Ba/Sr), natrium over kalium (Na/K), barium over titanium (Ba/Ti), manganese over titanium (Mn/

Ti) were examined, each presenting distinct characteristics in soil sampled from the 2004 Indian Ocean tsunami-affected regions. Following the 2011 Tohoku tsunami, previous studies revealed that soil samples collected from the Sendai plains in Tohoku, Japan exhibited a significant increase in the Na/Ti concentration ratio, which was twice as high as that

Table 2: The LIBS emission intensity ratio of chemical elements observed in soils sampled from tsunami-affected regions in multiple locations in Aceh Province, Indonesia

Sampling location	LIBS intensity emission ratio						Remarks
	Na/Ti	Ca/Ti	Mg/Ti	Al/Ti	Si/Ti	Ca/Fe	
	Na I	Ca II	Mg I	Al I	Si I	Ca II	
	588.85 nm	397.00 nm	518.57 nm	395.44 nm	288.10 nm	397.00 nm	
	Ti I	Ti I	Ti I	Ti I	Ti I	Fe I	
	334.70 nm	334.70 nm	334.70 nm	334.70 nm	334.70 nm	262.95 nm	
Banda Aceh 4 (A)	6	18	3	7	17	13	
Banda Aceh 5 (B)	5	14	3	8	16	6	
Banda Aceh 8 (C)	4	14	3	7	9	12	
Aceh Besar 1 (D)	6	14	3	6	21	8	
Aceh Besar 2 (E)	5	13	4	9	8	9	
Aceh Besar 3 (F)	5	13	4	7	13	7	
Aceh Besar 9 (G)	6	13	4	8	16	7	
Aceh Barat 4 (H)	6	13	5	5	7	12	
Aceh Barat 5 (I)	4	13	7	9	10	8	
Aceh Barat 6 (J)	4	15	6	7	23	8	
Aceh Barat 7 (K)	4	11	5	8	11	6	
Tungkob (L)	2	10	4	6	6	4	Unaffected soil
Pango Deah (M)	2	10	3	6	7	4	Unaffected soil
Blang Bintang (N)	2	10	2	6	7	4	Unaffected soil

Table 3: The LIBS emission intensity ratio of chemical elements observed in soils sampled from tsunami-affected regions in multiple locations in Aceh Province, Indonesia

Sampling location	LIBS intensity emission ratio						Remarks
	Ca/Mg	Ca/K	Ba/Sr	Na/K	Ba/Ti	Mn/Ti	
	Ca II	Ca II	Ba I	Na I	Ba I	Fe I	
	397.00 nm	397.00 nm	455.47 nm	588.85 nm	455.47 nm	262.95 nm	
	Mg I	K I	Sr I	K I	Ti I	Ti I	
	518.57 nm	766.90 nm	460.88 nm	766.90 nm	334.70 nm	334.70 nm	
Banda Aceh 4 (A)	6	18	1	2	1	1	
Banda Aceh 5 (B)	6	14	1	2	1	1	
Banda Aceh 8 (C)	5	14	1	1	1	1	
Aceh Besar 1 (D)	4	14	1	2	1	1	
Aceh Besar 2 (E)	5	13	1	2	1	1	
Aceh Besar 3 (F)	5	13	1	2	1	1	
Aceh Besar 9 (G)	4	13	1	1	1	1	
Aceh Barat 4 (H)	4	13	1	2	1	1	
Aceh Barat 5 (I)	4	13	1	3	1	1	
Aceh Barat 6 (J)	4	15	1	2	1	1	
Aceh Barat 7 (K)	4	11	1	2	1	1	
Tungkob (L)	2	10	1	1	1	1	Unaffected soil
Pango Deah (M)	2	10	1	1	1	1	Unaffected soil
Blang Bintang (N)	2	10	1	1	1	1	Unaffected soil

of the unaffected areas (Watanabe et al., 2020). The findings from this study are consistent with those of (Watanabe et al., 2020) which demonstrated a notable 2 to 3-fold increase in Na/Ti emission intensity ratio across tsunami-affected areas compared to unaffected regions. Hence, the Na/Ti ratio functions as a reliable chemical indicator for discerning the regions affected by the 2004 Indian Ocean tsunami. The Ca/Ti concentration comparison has emerged as a widely used indicator to differentiate chemical characteristics between marine and terrestrial environments (Willershauser et al., 2015; Donnelly et al., 2016). Findings from this study suggest that the emission intensity ratio of Ca/Ti in soils sampled from tsunami-affected regions was approximately double that of soils from areas not affected by tsunamis. This study also uncovered a notable elevation Mg/Ti and Si/Ti ratios, exhibiting values two to three times greater than those observed in soils sampled from tsunami-affected regions. The emission intensity ratios of Ca/K and Na/K are reported to double in soil sampled from tsunami-affected regions. Ba/Ti and Mn/Ti ratios exhibit identical values of 1 in both soil sampled from tsunami-affected and unaffected areas. The emission intensity ratios of Al/Ti, Ba/Sr, Na/K, Ba/Ti, and Mn/Ti, as reported in this study did not exhibit significant differences between soil sampled from tsunami-affected areas and those unaffected regions. In contrast, Na/Ti, Ca/Ti, Mg/Ti, Si/Ti, Ca/Fe, Ca/Mg, and Ca/K ratios displayed markedly distinct values across all soil sampled from tsunami-affected in Province of Aceh. Therefore, it can be inferred that these ratios act as reliable chemical indicators for detecting the flooding triggered by the 2004 Indian Ocean tsunami in Aceh Province.

CONCLUSION

The utilization of a pulsed CO₂ LIBS technique has undergone enhancements, modifications, and standardization to effectively detect and measure chemical constituents present in soil samples collected from the areas affected by the 2004 Indian Ocean tsunami in Aceh Province. Laser-induced plasma has been confirmed to achieve local thermal equilibrium in order to guarantee the precision of qualitative and quantitative analysis. A pulsed CO₂ LIBS successfully identifies a range of chemical elements, including salt elements (Ca, Al, Mg, Na, and K), metals (Ti, Fe, Si, Ba, Sr, Mn, Cr, Zn, Pb,

Cd, Cu, Co, Ni), and organic elements (C, H, O, N). A pulsed CO₂ laser analysis outperforms the Nd-YAG laser in identifying a wider range of elemental emission lines with high intensity-to-background ratios. It excels in detecting specific metal emission lines (Zn, Cr, Cu, Co, and Ni) which is challenging for Nd-YAG LIBS. The quantification of these elements can be performed using the CF-LIBS method, which consistently yields results similar to XRF. However, LIBS significantly outperforms XRF significantly as it has the capability to detect a wide range of elements, including light elements and certain heavy metals. Soil samples obtained from regions impacted by a tsunami exhibited a more than tenfold rise in the concentrations of salt elements and particular heavy metals when contrasted with soil samples from unaffected areas in 2006. Na levels surged from 0.02% to 4.18 - 4.95%, while Ca rose from 0.46% to 11.26 - 13.53%. The concentration of K increased from 0.11% to 5.50 - 6.96%, and Mg increased from 0.36% to 7.62 - 8.67%. The occurrence of this phenomenon is attributed to the accumulation of materials carried by tsunamis, such as saltwater and debris, leading to changes in the soil's structure and nutrient content. The investigation into emission intensity ratios using LIBS across multiple elements reveals noteworthy indicators, including Na/Ti, Ca/Ti, Mg/Ti, Si/Ti, Ca/Fe, Ca/Mg, and Ca/K. These ratios present compelling potential to differentiate between soils collected from the regions in Aceh Province that were impacted by the 2004 Indian Ocean tsunami and those that remained unaffected. This latest research underscores the exceptional promise of pulsed CO₂ LIBS as a rapid, efficient, and impactful technique for both qualitative and quantitative analysis of soils sampled from 2004 Indian Ocean tsunami-affected regions in Aceh Province. The potential future research directions in CO₂ LIBS for soil analysis, particularly in investigating the effects of natural disasters, include advancing precise and sensitive methodologies, the utilization of portable systems for real-time field monitoring and integration with early warning systems to improve preparedness and reduce risks associated with natural disasters.

AUTHOR CONTRIBUTIONS

R. Mitaphonna led sample collection, data analysis, and manuscript finalization. M. Ramli contributed

to the research design and data analysis. N. Ismail interpreted results and crafted discussion and result sections. K. Kurihara executed the experimental setup. K. Lahna conducted data analysis. N. Idris oversaw research coordination and article compliance.

ACKNOWLEDGEMENT

The authors gratefully acknowledge financial support from the Directorate of Research and Community Service, Ministry of Research, Technology, and Higher Education, Government of Indonesia, through PMDSU 2021 research Grant (contract number [53/UN11.2.1/PT.01.03/DPRM/2021] and Penelitian Dasar Unggulan Perguruan Tinggi (PDUPT), contract number: 84/UN11.2/PP/SP3/2019], as well as from the University of Fukui, Japan.

CONFLICT OF INTEREST

The authors declare that there is no conflict of interests regarding the publication of this manuscript. In addition, the ethical issues, including plagiarism, informed consent, misconduct, data fabrication and/or falsification, double publication and/or submission, and redundancy have been completely observed by the authors.

OPEN ACCESS

©2024 The author(s). This article is licensed under a Creative Commons Attribution 4.0 International License, which permits use, sharing, adaptation, distribution and reproduction in any medium or format, as long as you give appropriate credit to the original author(s) and the source, provide a link to the Creative Commons license, and indicate if changes were made. The images or other third-party material in this article are included in the article's Creative Commons license unless indicated otherwise in a credit line to the material. If material is not included in the article's Creative Commons license and your intended use is not permitted by statutory regulation or exceeds the permitted use, you will need to obtain permission directly from the copyright holder. To view a copy of this license, visit: <http://creativecommons.org/licenses/by/4.0/>

PUBLISHER'S NOTE

GJESM Publisher remains neutral with regard to jurisdictional claims in published maps and institutional affiliations.

ABBREVIATIONS

%	Percent
°C	Degree Celsius
μs	microsecond
$(U)_sT$	Partition function of species (s) at temperature (T),
$(U)T$	Partition function
A_k	Pre-exponential Factor
Al	Aluminium
Al/Ti	Aluminium over titanium
Ba	Barium
Ba/Sr	Barium over strontium
Ba/Ti	Barium over titanium
C	Carbon
Cd	Cadmium
Ca	Calcium
Ca/Fe	Calcium over iron
Ca/Mg	Calcium over magnesium
Ca/Ti	Calcium over titanium
CF	Chemical fraction representing the proportion of the element
CF-LIBS	Calibration-free laser-induced breakdown spectroscopy
CO ₂ -LIBS	Carbon dioxide laser-induced breakdown spectroscopy
cm	Centimeter
Co	Cobalt
Cr	Chromium
C_s	Concentration of species
Cu	Copper
EDS	Energy dispersive X-ray spectroscopy
E_k	Activation energy
FAAS	Flame atomic absorption spectrometry
Fe	Iron
Grooves/mm	Grooves per millimeter
G_k	State sum factor describing the total energy contributions
h	Hour
H	Hydrogen
Hz	Hertz

<i>I</i>	Total intensity of the detected element emission lines
<i>IC</i>	Ion Chromatography
<i>ICP</i>	Inductively coupled plasma
<i>INAA</i>	Instrumental neutron activation analysis
<i>J/pulse</i>	Joules per pulse
<i>K</i>	Potassium
<i>K/Ti</i>	Kalium over titanium
<i>K</i>	Kelvin
<i>k</i>	Boltzmann constant
<i>km</i>	kilometre
<i>LIBS</i>	Laser-induced breakdown spectroscopy
<i>Li</i>	Lithium
<i>LIP</i>	Laser-induced plasma
<i>ln</i>	Natural logarithm
<i>LTE</i>	Local thermodynamic equilibrium
<i>m</i>	meter
<i>Mg</i>	Magnesium
<i>Mg/Ti</i>	Magnesium over titanium
<i>Mn</i>	Manganese
<i>Mn/Ti</i>	Manganese over titanium
<i>Na</i>	Natrium
<i>Na/Ti</i>	Natrium over titanium
<i>Na/K</i>	Natrium over kalium
<i>Nd-YAG</i>	Neodymium-doped Yttrium Aluminum Garnet
<i>Ne</i>	Electron density
<i>Ni</i>	Nickel
<i>nm</i>	Nanometer
<i>ns</i>	Nanosecond
<i>O</i>	Oxygen
<i>Pb</i>	Lead
<i>Q_s</i>	Chemical potential of species (s)
<i>Si</i>	Silicon
<i>Si/Ti</i>	Silicon over titanium
<i>Sr</i>	Strontium
<i>T</i>	Temperature
<i>Te</i>	Electron temperature

<i>Ti</i>	Titanium
<i>XRF</i>	X-ray fluorescence
<i>Zn</i>	Zinc

REFERENCES

- Aldakheel, R.K.; Gondal, M.A.; Almessiere, M.A.; Rehman, S.; Nasr, M.M.; Alsalem, Z.; Khan, F.A., (2021). Spectrochemical analysis using libs and icp-oes techniques of herbal medicine (Tinnevely Senna leaves) and its anti-cancerous/antibacterial applications. *Arabian J. Chem.*, 14(12): 103451 (14 pages).
- Aldakheel, R.K.; Gondal, M.A.; Nasr, M.M.; Dastageer, M.A., (2021). Quantitative elemental analysis of nutritional , hazardous and pharmacologically active elements in medicinal Rhatany root using laser induced breakdown spectroscopy. *Arabian J. Chem.*, 14(2): 102919 (9 pages).
- Brunnbauer, L.; Gajarska, Z.; Lohninger, H.; Limbeck, A., (2023). A critical review of recent trends in sample classification using laser-induced breakdown spectroscopy (libs). *TrAC, Trends Anal. Chem.*, 159: 116859 (23 pages).
- Chaerun, S.K.; Whitman, W.B.; Wirth, S.J.; Ellerbrock, R.H., (2009). Chemical and mineralogical characterization of agricultural soils inundated by the December 26, 2004 tsunami after intrinsic bioremediation in Banda Aceh, Sumatra Island, Indonesia. *Journal of the American Society of Mining and Reclamation.*, 40502(30), 210-226 (17 pages).
- Chagué-goff, C.; Szczuci, W.; Shinozaki, T., (2017). Applications of geochemistry in tsunami research: A review. *Earth Sci. Rev.*, 165: 203–244 (42 pages).
- Ciucci, A.; Palleschi, V.; Rastelli, S.; Salvetti, A.; Singh, D.P.; Tognoni, E., (1999). CF-LIPS: A new approach to lips spectra analysis. *Laser Part. Beams.* 17(4): 793–797 (5 pages).
- Daly, P.; Halim, A.; Hundlani, D.; Ho, E., (2017). Rehabilitating coastal agriculture and aquaculture after inundation events : Spatial analysis of livelihood recovery in post-tsunami Aceh, Indonesia. *Ocean Coast. Manage.*, 142: 218–232 (15 pages).
- Donnelly, J.; Goff, J.; Chagué-goff, C., (2016). A record of local storms and trans-Pacific tsunamis, eastern Banks Peninsula, New Zealand. *The Holocene.* 1-13 (13 pages).
- Fayyaz, A.; Asghar, H.; Alshehri, A.M.; Alrebdi, T.A., (2023). LIBS assisted pca analysis of multiple rare-earth elements (La, Ce, Nd, Sm, and Yb) in phosphorite deposits. *Heliyon.* 9(3): e13957 (16 pages).
- Gouramanis, C.; Switzer, A.D.; Jankaew, K.; Bristow, C.S.; Pham, D.T.; Ildefonso, S.R., (2017). High-frequency coastal overwash deposits from Phra Thong Island, Thailand. *Nature.* 7: 43742 (9 pages).
- Hu, Z.; Zhang, D.; Wang, W.; Chen, F.; Xu, Y.; Nie, J.; Chu, Y.; Guo, L., (2022). A review of calibration-free laser-induced breakdown spectroscopy. *TrAC, Trends Anal. Chem.*, 152: 116618 (11 pages).
- Idris, N.; Gondal, M.A.; Lahna, K.; Ramli, M.; Sari, A.M.; Aldakheel, R.K.; Mitaphonna, R.; Dastageer, M.A.; Kurihara, K.; Kurniawan, K.H.; Almessiere, M.A., (2022). Geochemistry study of soil affected catastrophically by tsunami disaster triggered by 2004 Indian Ocean earthquake using a fourth harmonics (k = 266 nm) Nd:YAG laser induced breakdown spectroscopy. *Arabian J. Chem.*, 15(7): 103847 (12 pages).
- Ishizawa, T.; Goto, K.; Yokoyama, Y.; Miyairi, Y., (2019). Non-

- destructive analyses to determine appropriate stratigraphic level for dating of tsunami deposits. *Mar. Geol.*, 412: 19–26 **(8 pages)**.
- Khan, Z. H.; Ullah, M.H.; Rahman, B.; Talukder, A.I.; Wahadoszamen, Md.; Abedin, K.M.; Haider, A.F.M.Y., (2022). Laser-Induced Breakdown Spectroscopy (LIBS) for trace element detection: A Review. *J. Spectrosc.*, 3887038 **(25 pages)**.
- Khumaeni, A.; Budi, W.S.; Kurihara, K.; Kurniawan, H.; Kagawa, K., (2020). Trace metal analysis of element on material surface using pulse CO₂ laser-induced breakdown spectroscopy applying vaporization technique. *Heliyon*. 6(8): e04670 **(50 pages)**.
- Khumaeni, A.; Budi, W.S.; Lie, Z.S.; Kurniawan, K.H.; Kurihara, K.; Kagawa, K. (2018). Pulsed CO₂ laser-induced gas plasma spectroscopy based on single beam splitting for trace metal analysis on a material surface. *J. Mod. Opt.*, 65(19): 2229-2233 **(10 pages)**.
- Khumaeni, A.; Budi, W.S.; Kurniawan, K.; Fukumoto, K. I.; Kurihara, K.; Kagawa, K., (2022). Quantification of sodium contaminant on steel surfaces using pulse CO₂ laser-induced breakdown spectroscopy. *Arabian J. Chem.*, 15(1): 103474 **(7 pages)**.
- Legnaioli, S.; Campanella, B.; Poggialini, F.; Pagnotta, S.; Harith, M.A.; Abdel-Salam, Z.A.; Palleschi, V., (2020). Industrial applications of laser-induced breakdown spectroscopy: A review. *Anal. Methods*. 12(8): 1014–1029 **(16 pages)**.
- Liu, X.; Zhang, Q.; Wu, Z.; Shi, X.; Zhao, N.; Qiao, Y., (2015). Rapid elemental analysis and provenance study of *Blumea balsamifera* DC using laser-induced breakdown spectroscopy. *Sensors*, 15(1): 642-655 **(14 pages)**.
- Martínez-Mincheró, M.; Cobo, A.; Méndez-Vicente, A.; Pisonero, J.; Bordel, N.; Gutiérrez-Zugasti, I.; Roberts, P.; Arrizabalaga, Á.; Valdiande, J.; Mirapeix, J.; López-Higuera, J.M.; García-Escárgaza, A., (2023). Comparison of Mg/Ca concentration series from *Patella depressa* limpet shells using CF-LIBS and LA-ICP-MS., *Talanta*. 251: 123757 **(11 pages)**.
- Messenger, M.L.; Davies, I.P.; Levin, P.S., (2021). Development and validation of in-situ and laboratory X-ray fluorescence (xrf) spectroscopy methods for moss biomonitoring of metal pollution. *MethodsX*. 8: 101319 **(13 pages)**.
- Mitaphonna, R.; Ramli, M.; Ismail, N.; Idris, N., (2023). Evaluation of geochemical signature in soil sampled from a 2004 Indian Ocean tsunami-stricken region in Aceh Province located in the western part of Indonesia using scanning electron microscopy – energy dispersive x-ray (sem-edx) spectroscopy and its compatibility with x-ray fluorescence (xrf) measurement. *Phil. J. Sci.*, 152(1): 485–499 **(15 pages)**.
- Quackatz, L.; Gornushkin, I.; Griesche, A.; Kannengiesser, T.; Treutler, K.; Wesling, V., (2024). In situ chemical analysis of duplex stainless steel weld by laser induced breakdown spectroscopy. *Spectrochimica Acta Part B: At. Spectrosc.* 214: 106899 **(7 pages)**.
- Ravansari, R.; Wilson, S.C.; Tighe, M., (2020). Portable x-ray fluorescence for environmental assessment of soils : Not just a point and shoot method. *Environ. Int.*, 134: 05250 **(14 pages)**.
- Rehan, A.; Gondal, M.A.; Aldakheel, R.K.; Rehan, K.; Sultana, S.; Almessiere, M.A.; Ali, Z., (2021). Development of laser induced breakdown spectroscopy technique to study irrigation water quality impact on nutrients and toxic elements distribution in cultivated soil. *Saudi J. Biol. Sci.*, 28 (12): 6876-6883 **(8 pages)**.
- Shinozaki, T., (2021). Geochemical approaches in tsunami research: current knowledge and challenges. *Geosci. Lett.*, 8(1) **(13 pages)**.
- Shinozaki, T.; Sawai, Y.; Ikehara, M.; Matsumoto, D.; Shimada, Y.; Tanigawa, K.; Tamura, T., (2022). Identifying tsunami traces beyond sandy tsunami deposits using terrigenous biomarkers: a case study of the 2011 Tohoku - oki tsunami in a coastal pine forest, northern Japan. *Prog. Earth Planet. Sci.*, 9: 29 **(10 pages)**.
- Sulistiyowati, L.; Yolanda, Y.; Andareswari, N., (2023). Harbor water pollution by heavy metal concentrations in sediments. *Global J. Environ. Sci. Manage.*, 9(4): 885-898 **(14 pages)**.
- Szczuciński, W.; Niedzielski, P.; Kozak, L.; Frankowski, M.; Ziola, A.; Lorenc, S., (2007). Effects of rainy season on mobilization of contaminants from tsunami deposits left in a coastal zone of Thailand by the 26 December 2004 tsunami. *Environ. Geol.*, 53: 253–264 **(12 pages)**.
- Tripathi, D.K.; Pathak, A.K.; Chauhan, D.K.; Dubey, N.K.; Rai, A.K.; Prasad, R., (2015). An efficient approach of laser induced breakdown spectroscopy (libs) and icap-aes to detect the elemental profile of *Ocimum L.* species. *Biocatal. Agric. Biotechnol.*, 4(4): 471-479 **(10 pages)**.
- Villas-Boas, P.R.; Franco, M.A.; Martin-Neto, L.; Gollany, H.T.; Milori, D.M.B.P., (2020). Applications of laser-induced breakdown spectroscopy for soil characterization, part II: Review of elemental analysis and soil classification. *Eur. J. Soil Sci.*, 71, 805–818 **(14 pages)**.
- Watanabe, T.; Tsuchiya, N.; Yamasaki, S.; Sawai, Y., (2020). A geochemical approach for identifying marine incursions : Implications for tsunami geology on the Pacific coast of northeast Japan. *Appl. Geochem.*, 118: 104644 **(11 pages)**.
- Watanabe, T.; Kagami, S.; Niwa, M., (2022). Geochemical and heavy mineral signatures of marine incursions by a paleotsunami on the Miyazaki plain along the Nankai – Suruga trough, the Pacific coast of southwest Japan. *Mar. Geol.*, 444: 106704 **(13 pages)**.
- Willershäuser, T.; Vött, A.; Hadler, H.; Fischer, P.; Rübke, B.; Ntageretzis, K.; Emde, K.; Brückner, H. (2015). Geo-scientific evidence of tsunami impact in the Gulf of Kyparissia (western Peloponnese, Greece). *Borntraeger Verlag*. 59: 43–80 **(38 pages)**.
- Wisner, B.; Blaikie, P.; Cannon, T.; Davis, I., (2004). *At Risk: Natural Hazards, People's Vulnerability and Disasters*. Routledge.
- Yu, K.; Ren, J.; Zhao, Y., (2020). Principles, developments and applications of laser-induced breakdown spectroscopy in agriculture: A review. *Artif. Intell. Agric.*, 4: 127–139 **(13 pages)**.
- Zakaly, H.M.H.; Uosif, M.A.M.; Issa, S.A.M.; Tekin, H.O.; Madkour, H.; Tammam, M.; El-Taher, A.; Alharshan, G.A.; Mostafa, M.Y.A., (2021). An extended assessment of natural radioactivity in the sediments of the mid-region of the Egyptian Red Sea coast. *Mar. Pollut. Bull.*, 171: 112658 **(12 pages)**.
- Zivkovic, S.; Savovic, J.; Kuzmanovic, M.; Petrovic, J.; Momcilovic, M., (2018). Alternative analytical method for direct determination of Mn and Ba in peppermint tea based on laser-induced breakdown spectroscopy. *Microchem. J.*, 137: 410-417 **(18 pages)**.

AUTHOR (S) BIOSKETCHES

Mitaphonna, R., Ph.D. Candidate, Graduate School of Mathematics and Applied Sciences, Universitas Syiah Kuala, Jl. Professor Dr. Ibrahim Hasan, Gampong Pie, Indonesia.

- Email: Rara2019@mhs.unsyiah.ac.id
- ORCID: 0009-0008-4360-9269
- Web of Science ResearcherID: KYC-3037-2024
- Scopus Author ID: 57212673530
- Homepage: <https://raramitaphonna.wordpress.com/>

Idris, N., Ph.D., Professor, Physics Department, Universitas Syiah Kuala, Jl. Tgk.Syech Abdur Rauf No. 3, Darussalam, Banda Aceh, Indonesia.

- Email: nasrullah.idris@usk.ac.id
- ORCID: 0000-0002-1650-8365
- Web of Science ResearcherID: K-6292-2015
- Scopus Author ID: 6603916218
- Homepage: <https://fsd.usk.ac.id/nasrullahidris/>

Ramli, M., Ph.D., Associated Professor, Chemistry Department, Universitas Syiah Kuala, Jl. Tgk.Syech Abdur Rauf No. 3, Darussalam, Banda Aceh, Indonesia.

- Email: muliadiramli@usk.ac.id
- ORCID: 0000-0003-1564-7088
- Web of Science ResearcherID: GPP-3267-2022
- Scopus Author ID: 16231194500
- Homepage: <https://fsd.usk.ac.id/muliadiramli/>

Ismail, N., Ph.D., Professor, Geophysical Department, Universitas Syiah Kuala, Jl. Tgk.Syech Abdur Rauf No. 3, Darussalam, Banda Aceh, Indonesia.

- Email: nazli.ismail@usk.ac.id
- ORCID: 0000-0002-7136-2186
- Web of Science ResearcherID: R-1048-2017
- Scopus Author ID: 35193985000
- Homepage: <https://geologi.usk.ac.id/id/nazli-ismail-ssi-msi-phd>

Kurihara, K., Ph.D., Professor, Physics Department, University of Fukui, Bunkyo, Fukui 910-8507, Japan.

- Email: kuri@u-fukui.ac.jp
- ORCID: 0009-0004-9085-7426
- Web of Science ResearcherID: NA
- Scopus Author ID: 7201617094
- Homepage: <https://r-info.ad.u-fukui.ac.jp/Profiles/3/0000214/profile.html?lang=en>

Lahna, K., Ph.D., Associated Professor, Physics Department, Universitas Syiah Kuala, Jl. Tgk.Syech Abdur Rauf No. 3, Darussalam, Banda Aceh, Indonesia.

- Email: kurnialahna@usk.ac.id
- ORCID: 0000-0001-8263-6237
- Web of Science ResearcherID: GPS-8330-2022
- Scopus Author ID: 6503980251
- Homepage: <https://fsd.usk.ac.id/kurnialahna/>

HOW TO CITE THIS ARTICLE

Mitaphonna, R.; Idris, N.; Ramli, M. Ismail, N.; Kurihara, K.; Lahna, K., (2024). A pulsed carbon dioxide laser induced breakdown analysis for chemical profile of tsunami affected soil. *Global J. Environ. Sci. Manage.*, 10(3): 1211-1226.

DOI: [10.22034/gjesm.2024.03.17](https://doi.org/10.22034/gjesm.2024.03.17)

URL: https://www.gjesm.net/article_712407.html

